Biscale chaos in propagating fronts

Anatoly Malevanets, Agustí Careta,* and Raymond Kapral
Chemical Physics Theory Group, Department of Chemistry, University of Toronto, Toronto, Canada M5S 1A1
(Received 25 May 1995)

The propagating chemical fronts found in cubic autocatalytic reaction-diffusion processes are studied. Simulations of the reaction-diffusion equation near to and far from the onset of the front instability are performed and the structure and dynamics of chemical fronts are studied. Qualitatively different front dynamics are observed in these two regimes. Close to onset the front dynamics can be characterized by a single length scale and described by the Kuramoto-Sivashinsky equation. Far from onset the front dynamics exhibit two characteristic lengths and cannot be modeled by this amplitude equation. An amplitude equation is proposed for this biscale chaos. The reduction of the cubic autocatalysis reaction-diffusion equation to the Kuramoto-Sivashinsky equation is explicitly carried out. The critical diffusion ratio δ_c, where the planar front loses its stability to transverse perturbations, is determined and found to be $\delta_c = 2.300$.

PACS number(s): 05.45.+b, 82.40.Ck, 47.20.Ky

I. INTRODUCTION

Propagating fronts separating regions with different characteristics occur in many physical contexts. Often such fronts have a complicated structure of their own as in the fractal forms that arise in some diffusion-limited aggregration processes or viscous fingering [1]. In this paper we consider chemical fronts separating regions of distinctly different chemical concentrations and study the nature of the spatio-temporal dynamics that these fronts exhibit. In these systems, under appropriate conditions, a planar front may not be stable and complex, even chaotic, front dynamics can arise. For example, this is the situation often encountered in propagating flame fronts which have been studied extensively [2]. The complex dynamics of fronts can also underlie and determine the character of spatio-temporal chaos and dynamics in a variety of other chemical contexts [3].

We study a specific system here, the fronts in the cubic autocatalysis reaction $A + 2B \rightarrow 3B$, but several parts of our analysis are general and should apply in other situations. These cubic autocatalysis fronts have many features in common with propagating flames [4]. An experimental realization of such chemical front instabilities occurs in the iodate-arsenous acid reaction carried out in a gelled medium to suppress fluid flow [5]. The experiments show patterned fronts, much like those in quadratic and cubic mixed-order models.

For the cubic autocatalysis model, when the diffusion coefficient of the fuel A is sufficiently larger than that of the autocatalyst B, the planar front is unstable to transverse perturbations. We have investigated the nature of the resulting front dynamics as a function of the diffusion ratio D_A/D_B in large systems. Several results have emerged from our study of this system. For small enough diffusion ratios within the unstable regime the front exhibits complicated dynamics with statistically stationary properties and is characterized by a single length scale. Far beyond the instability point another chaotic regime is encountered, termed biscale chaos, in which there are two characteristic length scales.

We have carried out a detailed analysis of the front dynamics in terms of amplitude equations. Just beyond the instability threshold the front dynamics is described in terms of the Kuramoto-Sivashinsky equation [6,7]. We document this relation through a statistical characterization of the interface. The regime far from the instability point where biscale chaos is observed cannot be described in terms of the Kuramoto-Sivashinsky equation and we construct an amplitude equation in which the nonlinear mode coupling is generalized. This amplitude equation is able to capture the principal qualitative features of the biscale chaos. This part of the analysis may generalize to other situations.

We also give a detailed reduction of the cubic autocatalysis reaction-diffusion equation to the Kuramoto-Sivashinsky equation. The coefficients that enter in this equation are estimated analytically using solutions for the right and left eigenvectors of the eigenvalue problem that enters the analysis, and a numerical scheme is devised that allows the computation of these coefficients for any values of the diffusion coefficients. As a by-product of this analysis we may easily determine the critical diffusion ratio where the planar front becomes unstable.

II. CUBIC AUTOCATALYSIS FRONTS

Consider the autocatalytic reaction $A + 2B \longrightarrow 3B$ described by the reaction-diffusion equation

$$\frac{\partial \alpha}{\partial t} = -\alpha\beta^2 + D_A \Delta \alpha \,,$$

*Permanent address: Departament de Química Física, Universitat de Barcelona, Diagonal 647, E-08028 Barcelona, Spain.

$$\frac{\partial \beta}{\partial t} = \alpha\beta^2 + D_B \Delta\beta \,, \tag{1}$$

where $\alpha(t, \mathbf{r})$ and $\beta(t, \mathbf{r})$ are the (scaled) concentrations of the A and B species, respectively, with diffusion coefficients D_A and D_B. In one dimension, with suitably defined initial conditions [8], this system supports isothermal chemical fronts [9].

In two space dimensions the planar front is unstable to transverse perturbations when D_A is sufficiently larger than D_B. The origin of such instabilities and the nature of the resulting front dynamics have been the subject of earlier studies [4]. Horváth *et al.* [10] performed simulations of the cubic autocatalysis model (1) and investigated the bifurcation structure as a function of the system length. For small system sizes, when the front possesses a single minimum, the onset of chaotic behavior was observed to occur through a period doubling cascade in the temporal dynamics of the minimum. For large system sizes the resulting front dynamics is best analyzed in statistical terms. We now briefly describe and quantitatively characterize the nature of the front dynamics for large system lengths as a function of the diffusion coefficient ratio, $\delta = D_A/D_B$.

We consider a two-dimensional system which is infinite in the x direction and has length L along y, where periodic boundary conditions are applied. The initial conditions are taken to be $\{\alpha(0,x,y) = 1,\ \beta(0,x,y) = 0 \mid x \le -w/2, \forall y\}$ and $\{\alpha(0,x,y) = 0,\ \beta(0,x,y) = 1 \mid x \ge w/2, \forall y\}$. The region $\{x, y \mid -w/2 < x < w/2, 0 \le y \le L\}$ was divided into segments of length ℓ along y and each segment was assigned the values $(\alpha(0,x,y), \beta(0,x,y))$=(1,0) or (0,1) with probability $p = 1/2$. It is convenient to represent the front dynamics in terms of the isoconcentration profiles, $h_A(t,y)$ and $h_B(t,y)$ defined by $\alpha(t, h_A(t,y), y) = \alpha_r$ and $\beta(t, h_B(t,y), y) = \beta_r$, where α_r and β_r are reference concentrations. Henceforth we focus on $h_B(t,y)$ measured relative to its average value at time t and denote this quantity by $h(t,y)$. We note that for these initial conditions this average value moves with the minimum front speed, which is selected from the continuum of allowed front speed values.

Figure 1(a) shows a space-time plot of the minima of $h(t,y)$ for $\delta = 5$. In the integration [11] of (1) we have scaled the length variables so that $D_A = 1$ and $D_B = \delta^{-1}$. After an initial transient period during which the interface develops, a moving front with statistically stationary properties is formed. In this stationary regime the spatio-temporal behavior can be described in terms of the dynamics of the minima which play the role of "particles" in the system. The particles collide and coalesce and new particles are born so that the average density of particles per unit length remains constant. The front dynamics may be characterized quantitatively by the space-time correlation function

$$C(t,y) = \left\langle L^{-1} \int_0^L dy' [h(t,y') - h(t,y+y')]^2 \right\rangle \,, \tag{2}$$

where the angle brackets signify an average over realizations of the front evolution starting from the random initial conditions given above. We also consider the time average of $C(t,y)$ in the stationary regime,

$$\bar{C}(y) = T^{-1} \int_{t_0}^{t_0+T} dt'\ C(t',y) \,, \tag{3}$$

where t_0 is a time longer than the transient period. The correlation function (2) is sketched in Fig. 2 for several values of the time t and shows the development of correlations during the transient period and the approach to the stationary regime. The function $C(t,y)$ exhibits short range correlations with a tendency to reach a nearly parabolic form, seen in the $\bar{C}(y)$ curve, which is characteristic of diffusive transverse front dynamics and will be discussed further below. The persistent short range correlations are due to the existence of a characteristic length ℓ^* arising from the front instability.

This type of behavior persists up to about $\delta = 6$ when a new type of chaotic front dynamics, distinguished by the appearance of a second length scale, is observed. The second length scale is easily discerned in both the space-time plot of the minima of $h(t,y)$ shown in Fig. 1(b) for

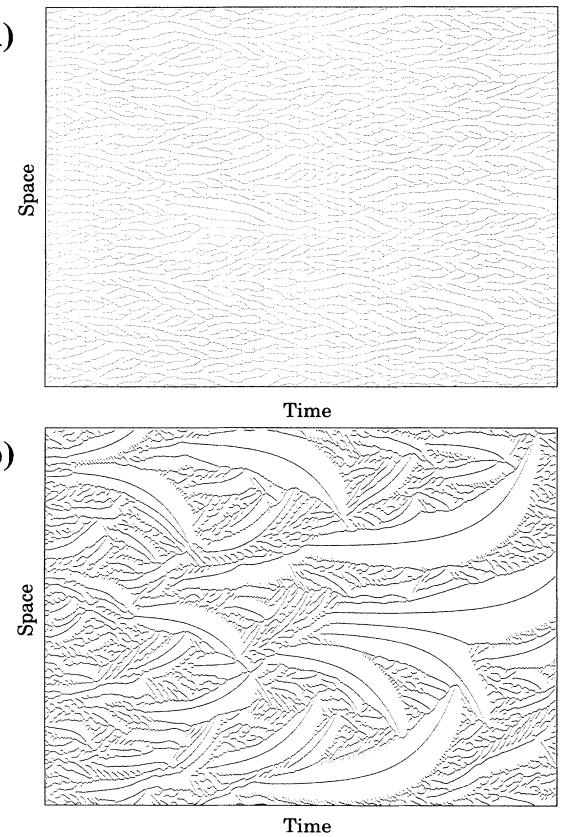

FIG. 1. Panels (a) and (b) are space-time plots of the minima of the autocatalyst (B) profiles for the diffusion coefficient ratios $\delta = 5$ and $\delta = 8$, respectively. The isoconcentration level for these plots is $\beta_r = 0.5$. The ordinates range from 0 to L, where the system size is $L = 2048$. In the abscissas the initial time is $t = 0$ and the final time is $t = 100\,000$ for (a) and $t = 200\,000$ for (b).

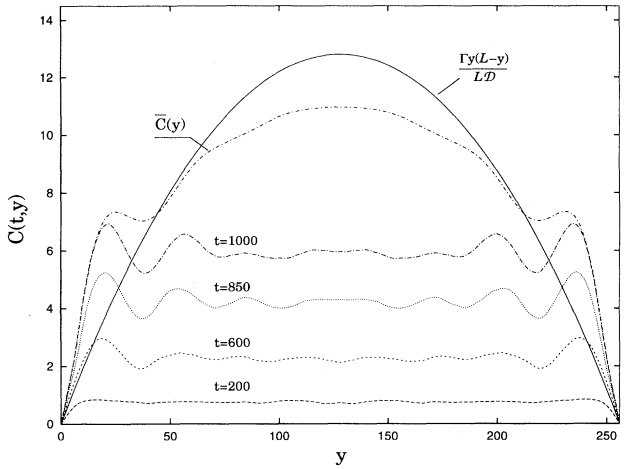

FIG. 2. The figure shows $C(t,y)$ for $\delta = 5$ for several values of t indicated on the plot, as well as $\bar{C}(y)$ and the theoretical value of $\bar{C}(y) = \Gamma y(L-y)/\mathcal{D}L$ for a diffusive interface where nonlinear terms in the Kardar-Parisi-Zhang equation can be neglected. The parameter $\bar{\mathcal{D}} = \Gamma/\mathcal{D}$, determined from a fit to the $\bar{C}(y)$ data, has the value $\bar{\mathcal{D}} \approx 0.2$. The parameter Γ may be estimated independently from the linear growth of the $k = 0$ Fourier mode. Its value was found to be $\Gamma \approx 0.018$. Fronts corresponding to the isoconcentration lines $\beta_r = 0.5$ were used to construct these correlation functions. The system length was $L = 256$ and $C(t,y)$ was determined from an average over 25 realizations of the front evolution. In the computation of $\bar{C}(y)$, we used $t_0 = 25\,000$ and $t_0 + T = 50\,000$.

$\delta = 8$ and the power spectrum,

$$E(k) = T^{-1} \int_{t_0}^{t_0+T} dt \langle |h(t,k)|^2 \rangle \ . \tag{4}$$

The power spectrum is presented in Fig. 3 for both $\delta = 5$

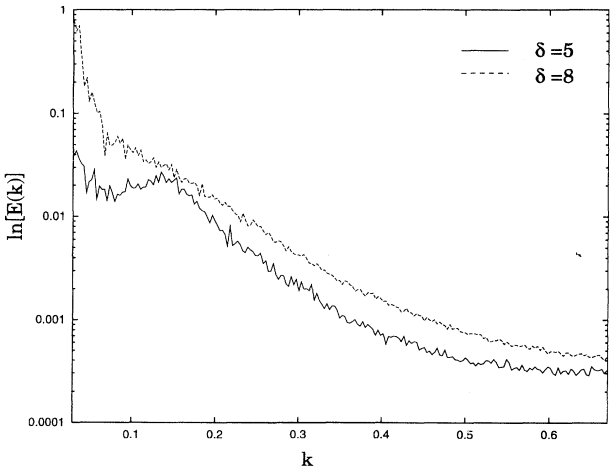

FIG. 3. Power spectra for $\delta = 5$ and $\delta = 8$. The isoconcentration lines for $\beta_r = 0.5$ were used to construct these power spectra. The system length was $L = 2048$ and $E(k)$ was determined from a single run of the front evolution. For $\delta = 5$ we used $t_0 = 25\,000$ and $t_0 + T = 100\,000$, while for $\delta = 8$ we used $t_0 = 50\,000$ and $t_0 + T = 200\,000$.

and $\delta = 8$. For $\delta = 5$ one sees a single peak corresponding to the wave number of the most unstable mode. However, for $\delta = 8$ the minimum in the power spectrum has filled in, indicating the growth of modes with smaller wave numbers and thus the appearance of structure on longer length scales. We now turn to an analysis of these results in terms of amplitude equations and provide a foundation for the phenomenological picture of the front dynamics.

III. ANALYSIS OF FRONT DYNAMICS

A description of the origin of the front dynamics is most conveniently given in terms of amplitude equations for the front profile derived from the reaction-diffusion equation (1). We analyze the dynamics close to the instability point in terms of the Kuramoto-Sivashinsky equation and show how this equation must be generalized in order to explain the regime far beyond the instability where a second characteristic length appears.

A. Dynamics of small perturbations

We present an adaptation of Kuramoto's derivation [12] for the case of small-amplitude perturbations which yields the amplitude equation that will be used in the subsequent analyses. We shall confine our attention to the question of how the presence of a second dimension affects the dynamics of the general reaction-diffusion system,

$$\frac{\partial \mathbf{z}}{\partial t} = \mathbf{F}(\mathbf{z}) + \mathbf{D}\Delta\mathbf{z} \ . \tag{5}$$

Here $\mathbf{z}$ is a vector of concentration fields and $\mathbf{F}(\mathbf{z})$ is a vector-valued function describing chemical reactions. We assume that in one dimension (5) possesses a stable solution with a propagating front profile $\mathbf{z}(t,x,y) = \mathbf{z}_0(x-ct)$, where c is the velocity of the front. Following the treatment by Kuramoto [12] we seek the dynamics of a perturbed solution in the form

$$\mathbf{z}(t,x,y) = \mathbf{z}_0(\xi + \phi_0(t,y)) + \sum_{i>0} \phi_i(t,y)\mathbf{u}_i(\xi) \ , \tag{6}$$

where $\xi = x - ct$. As is customary, we use an abstract notation $\langle \xi | \mathbf{u}_i \rangle = \mathbf{u}_i(\xi)$. The vectors $|\mathbf{u}_i\rangle$ are the solutions of the eigenvalue problem,

$$\left[\mathcal{D}\hat{\mathbf{F}}(\mathbf{z}_0) + \mathbf{D}\frac{\partial^2}{\partial \hat{\xi}^2} + c\frac{\partial}{\partial \hat{\xi}} \right] |\mathbf{u}_i\rangle \equiv \hat{\mathcal{L}}|\mathbf{u}_i\rangle = \lambda_i |\mathbf{u}_i\rangle \ , \tag{7}$$

where $\mathcal{D}\mathbf{F}$ is the Jacobian of the vector function $\mathbf{F}$ and $\hat{\mathcal{L}}$ is the operator in square brackets. Here a caret signifies an abstract operator while the corresponding quantity without a caret is its ξ representation. We expand $\mathbf{F}(\mathbf{z})$ in a Taylor series near $\mathbf{z}_0$ and neglect terms of second order and higher. Since the main features of the front dynamics are embodied in $\mathcal{D}\mathbf{F}$, the truncation of the Taylor series does not discard any important information. Due

to the translational symmetry of equation (5) we have a straightforward solution of (7), namely $|\mathbf{u}_0\rangle = \partial|\mathbf{z}_0\rangle/\partial\hat{\xi}$ corresponding to a zero eigenvalue. Taking this solution into account we write

$$\frac{\partial\phi_i}{\partial t}|\mathbf{u}_i\rangle = c|\mathbf{u}_0\rangle + \hat{\mathbf{F}}(\mathbf{z}_0) + \mathbf{D}\frac{\partial^2}{\partial\hat{\xi}^2}\mathbf{z}_0 + (\nabla\phi_0)^2\,\mathbf{D}\frac{\partial}{\partial\hat{\xi}}|\mathbf{u}_0\rangle + \Delta\phi_i\mathbf{D}|\mathbf{u}_i\rangle + \sum_{i>0}\phi_i\left[\mathcal{D}\mathbf{F}|\mathbf{u}_i\rangle + \mathbf{D}\frac{\partial^2}{\partial\hat{\xi}^2}|\mathbf{u}_i\rangle + c\frac{\partial}{\partial\hat{\xi}}|\mathbf{u}_i\rangle\right]. \tag{8}$$

Using the identity $-c|\mathbf{u}_0\rangle = \mathbf{F}(\mathbf{z}_0) + \mathbf{D}(\partial^2/\partial\hat{\xi}^2)|\mathbf{z}_0\rangle$ and definition (7) we arrive at the expression

$$\frac{\partial\phi_i}{\partial t}|\mathbf{u}_i\rangle = \lambda_i\phi_i|\mathbf{u}_i\rangle + \Delta\phi_i\mathbf{D}|\mathbf{u}_i\rangle + (\nabla\phi_0)^2\,\mathbf{D}\frac{\partial}{\partial\hat{\xi}}|\mathbf{u}_0\rangle\,. \tag{9}$$

Here and below we use the Einstein summation convention. Alternatively, after multiplication by $\langle\mathbf{u}_i|$, (9) may be represented by a set of coupled equations

$$\frac{\partial\phi_i}{\partial t} = \lambda_i\phi_i + \langle\mathbf{u}_i|\mathbf{D}|\mathbf{u}_j\rangle\Delta\phi_j + \langle\mathbf{u}_i|\mathbf{D}\frac{\partial}{\partial\hat{\xi}}|\mathbf{u}_0\rangle\,(\nabla\phi_0)^2\,. \tag{10}$$

This set of equations can be formally solved for modes ϕ_i ($i \neq 0$) by treating ϕ_0 as an independent function and applying Duhamel's principle to the resulting system of inhomogeneous linear equations. We find

$$\boldsymbol{\phi}(t) = e^{\widehat{\mathbf{W}}t}\boldsymbol{\phi}(0) + \int_0^t ds e^{\widehat{\mathbf{W}}(t-s)}[\mathbf{a}\Delta\phi_0(s) + \mathbf{b}[\nabla\phi_0(s)]^2]\,. \tag{11}$$

In (11) we use the following notation: the matrix operator $\widehat{\mathbf{W}}$ has elements $\widehat{W}_{ij} = \delta_{ij}\lambda_i + \langle\mathbf{u}_i|\mathbf{D}|\mathbf{u}_j\rangle\Delta$, the vectors $\mathbf{a}$ and $\mathbf{b}$ have elements $a_i = \langle\mathbf{u}_i|\mathbf{D}|\mathbf{u}_0\rangle$, $b_i = \langle\mathbf{u}_i|\mathbf{D}(\partial/\partial\hat{\xi})|\mathbf{u}_0\rangle$, respectively, and $\boldsymbol{\phi}$ is a vector with elements ϕ_i ($i > 0$).

Assuming that $\exp(\widehat{\mathbf{W}}t)$ decays rapidly compared to ϕ_0 we may perform the integration in (11) and substitute the result into the equation for ϕ_0 to obtain

$$\frac{\partial\phi_0}{\partial t} = \left(a_0 - \sum_{i,j>0} c_i\{\widehat{\mathbf{W}}^{-1}\}_{ij}a_j\Delta\right)\Delta\phi_0 + \left(b_0 - \sum_{i,j>0} c_i\{\widehat{\mathbf{W}}^{-1}\}_{ij}b_j\Delta\right)(\nabla\phi_0)^2\,, \tag{12}$$

where $c_i = \langle\mathbf{u}_0|\mathbf{D}|\mathbf{u}_i\rangle$. This is the generalized amplitude equation which will form the basis of the analysis of the biscale front chaos given below.

If the dynamics is described by small k modes one can take $\widehat{\mathbf{W}}^{-1}$ to be a diagonal matrix δ_{ij}/λ_i and by omitting second order terms in the coefficient of $(\nabla\phi)^2$ one obtains [13]

$$\frac{\partial\phi_0}{\partial t} = \langle\mathbf{u}_0|\mathbf{D}|\mathbf{u}_0\rangle\Delta\phi_0 + \langle\mathbf{u}_0|\mathbf{D}\frac{\partial}{\partial\hat{\xi}}|\mathbf{u}_0\rangle\,(\nabla\phi_0)^2 - \sum_{i>0}\frac{\langle\mathbf{u}_0|\mathbf{D}|\mathbf{u}_i\rangle\langle\mathbf{u}_i|\mathbf{D}|\mathbf{u}_0\rangle}{\lambda_i}\Delta^2\phi_0\,. \tag{13}$$

The coefficient of the $(\nabla\phi_0)^2$ term is obtained from the following identity:

$$0 \equiv \int_{-\infty}^{x}\left[\langle\mathbf{u}_0|\hat{\mathcal{L}}|\xi\rangle\langle\xi|\mathbf{u}_0\rangle - \langle\mathbf{u}_0|\xi\rangle\langle\xi|\hat{\mathcal{L}}|\mathbf{u}_0\rangle\right]d\xi = \left[2\langle\mathbf{u}_0|\xi\rangle\langle\xi|\mathbf{D}\frac{\partial}{\partial\hat{\xi}}|\mathbf{u}_0\rangle + \left(c - \mathbf{D}\frac{\partial}{\partial\xi}\right)\langle\mathbf{u}_0|\xi\rangle\langle\xi|\mathbf{u}_0\rangle\right]\Bigg|_x\,. \tag{14}$$

The above formula vanishes for all x so that after integrating over the entire domain we obtain $\langle\mathbf{u}_0|\mathbf{D}(\partial/\partial\hat{\xi})|\mathbf{u}_0\rangle = -c/2$ and observe that the expression has a universal character. This gives the Kuramoto-Sivashinsky equation

$$\frac{\partial\phi_0}{\partial t} = \nu\Delta\phi_0 - \frac{c}{2}(\nabla\phi_0)^2 - \kappa\Delta^2\phi_0\,, \tag{15}$$

with

$$\nu = \langle\mathbf{u}_0|\mathbf{D}|\mathbf{u}_0\rangle \tag{16}$$

and

$$\kappa = \sum_{i>0}\frac{\langle\mathbf{u}_0|\mathbf{D}|\mathbf{u}_i\rangle\langle\mathbf{u}_i|\mathbf{D}|\mathbf{u}_0\rangle}{\lambda_i}\,. \tag{17}$$

A stability analysis of (10) shows that the planar front is unstable with respect to long-scale, small-amplitude perturbations when $\nu < 0$.

In the next subsection we analyze the cubic autocatalysis front dynamics in terms of both the generalized amplitude equation (12) as well as the Kuramoto-Sivashinsky equation (15).

B. Amplitude equation description of front dynamics

1. *Dynamics near instability*

The Kuramoto-Sivashinsky equation provides insight into the nature of the cubic autocatalysis fronts close to the instability point, and we briefly comment on this connection. Simulations of the Kuramoto-Sivashinsky equation produce height correlation functions and space-time plots [cf. Fig. 4(a)] of the front dynamics similar to those of the cubic autocatalysis model. In terms of the Kuramoto-Sivashinsky equation, one sees that the front dynamics for $\delta > \delta_c$ is determined by the instability at long wavelengths, due to the fact that $\nu < 0$ in the $\Delta\phi_0$ term, and the dissipation at short wavelengths controlled by the $\Delta^2\phi_0$ term with positive κ. The dispersion relation of the Kuramoto-Sivashinsky equation is $\omega(k) = -\nu k^2 - \kappa k^4$ with maximum at $k_m = (-\nu/2\kappa)^{1/2}$. The long wavelength structure drives the dynamics of the extrema ("particles") whose collision dynamics provides

the dissipation of the energy. The characteristic distance between extrema can be related to the wave vector by $\ell^* = 2\pi/k_m$. Using a zeroth order approximation to the ν and κ coefficients given in the next section, for $\delta = 5$ we obtain $\ell^* = 30$ which is comparable to the value of $\ell^* = 39$ found in the numerical simulations. Using the methods given in Sec. IV it is possible to obtain ν and κ accurately and improve this estimate. For the present purposes this rough estimate plus the appearance of the space-time plot [14] in Fig. 4 suffice to confirm the general character of the Kuramoto-Sivashinsky mechanism for the chaotic cubic autocatalysis front dynamics for large system lengths.

It has been argued [15] that the long-scale dynamics of the one-dimensional Kuramoto-Sivashinsky equation can be described by the Kardar-Parisi-Zhang equation [16],

$$\frac{\partial \phi_0(t,y)}{\partial t} = \mathcal{D}\frac{\partial^2 \phi_0(t,y)}{\partial y^2} + \frac{c}{2}[\nabla \phi_0(t,y)]^2 + \xi(t,y) \ , \quad (18)$$

where c is the front speed, $\mathcal{D}$ is a diffusion coefficient, and $\xi(t)$ is a Gaussian white noise source with correlation function $\langle \xi(t,y)\xi(t',y')\rangle = 2\Gamma\delta(t-t')\delta(y-y')$. Although there is debate about some aspects of the reduction in higher dimensions [17], numerical simulations [18] of the scaling properties of the Kuramoto-Sivashinsky equation have confirmed this reduction in one dimension. The diffusive character of the cubic autocatalysis front dynamics discussed in Sec. II is consistent with such a description and provides additional confirmation of the applicability of the Kuramoto-Sivashinsky equation close to the onset of instability.

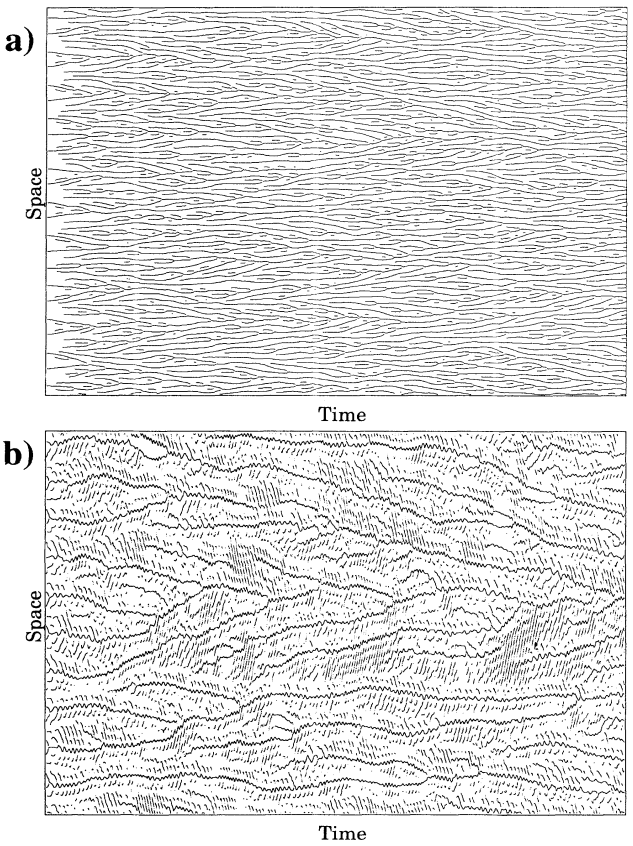

FIG. 4. Space-time plot of the minima of the profiles for (a) the Kuramoto-Sivashinsky equation and (b) the amplitude equation (19).

2. *Biscale chaos far from instability*

Far from instability, for $\delta \gg \delta_c$, we have seen that the cubic autocatalysis model presents new features. The space-time plot [Fig. 1(b)] shows that besides the relatively short-lived trajectories, which are similar to those of the Kuramoto-Sivashinsky equation, there exist long-lived, stable patterns. We have verified that this type of biscale chaotic front dynamics, which involves a second characteristic length scale, cannot be described by the Kuramoto-Sivashinsky equation. One may seek a generalization of the Kuramoto-Sivashinsky equation in which the coefficients of the $\Delta\phi_0$ and $\Delta^2\phi_0$ terms are modified; this in effect changes the dispersion relation and if it has the form sketched in Fig. 5(a) with two extrema then one might observe biscale spatio-temporal dynamics. We note, however, that direct numerical calculation of the fastest growth mode and the growth rate corresponding to it (cf. the Appendix for the method used to carry out this calculation) shows that the dispersion relation remains similar to that of the Kuramoto-Sivashinsky equation even for $\delta \gg \delta_c$ (see Fig. 5 for a schematic representation of the situation). Thus one must seek a description of this new type of front dynamics outside the usual Kuramoto-Sivashinsky equation or modifications of it that involve a generalized dispersion relation.

We now describe a model that captures the qualitative features of this phenomenon and is consistent with the amplitude equation (12) derived above. Since the origin of the new dynamics does not reside in terms that affect the dispersion relation, one is led to examine the nonlinear term in (12) which, for future reference, we rewrite in terms of its Fourier transform:

$$\frac{\partial \phi_0(t,k)}{\partial t} = \omega(k)\phi_0(t,k) + \frac{cg(k)}{4\pi}\sum_{k'} k'(k-k')\phi_0(t,k')\phi_0(t,k-k') \ , \quad (19)$$

where $g(k)$ is given by

$$-\frac{c}{2}g(k) = b_0 - \sum_{i,j>0} c_i\{\widehat{\mathbf{W}}(k)^{-1}\}_{ij}b_j k^2 \ . \quad (20)$$

Recall that $b_0 = -c/2$. The dynamical system governed by $\partial\phi/\partial t = (\nabla\phi)^2$ conserves the quantity $\int(\nabla\phi)^2 d\xi$ as can be seen easily from the identity [19]:

$$\frac{d}{d\tau}\int(\nabla\phi)^2 d\xi = -2\int \nabla^2\phi(\nabla\phi)^2 d\xi = -\frac{2}{3}\int \nabla(\nabla\phi)^3 d\xi \ , \quad (21)$$

so that below we shall refer to the linear and nonlinear terms in (19) as dissipation and mixing terms, respectively. Multiplying (19) by $\phi_0(t,-k)$ and averaging the resulting equation over time we have for the stationary power spectrum

$$0 = \omega(k)E(k) + \frac{cg(k)}{4\pi}\sum_{k'} k'(k-k') \times \langle \phi_0(t,k')\phi_0(t,k-k')\phi_0(t,-k)\rangle \ . \quad (22)$$

From this equation it is clear that the stationary properties depend on the ratio $\omega(k)/g(k)$ so that for $g(k)$ as in Fig. 5(b) we see that the growth of the mode with wave number k_0 is strongly suppressed. While the above arguments do not constitute a rigorous "proof" they serve as a guide to the proper form of the mixing coefficient. Technically, the above scheme is accomplished in a natural way when a zero of $\widehat{\mathbf{W}}(k)$ comes close to the real axis in the vicinity of the maximum of the dispersion relation. In this case the behavior of $g(k)$ is dominated by the pole of $\widehat{\mathbf{W}}^{-1}(k)$ and the mixing coefficient may be approximated by

$$g(k) = 1 + \frac{\epsilon k^2}{(k-k_0)^2+\gamma^2} \ , \quad (23)$$

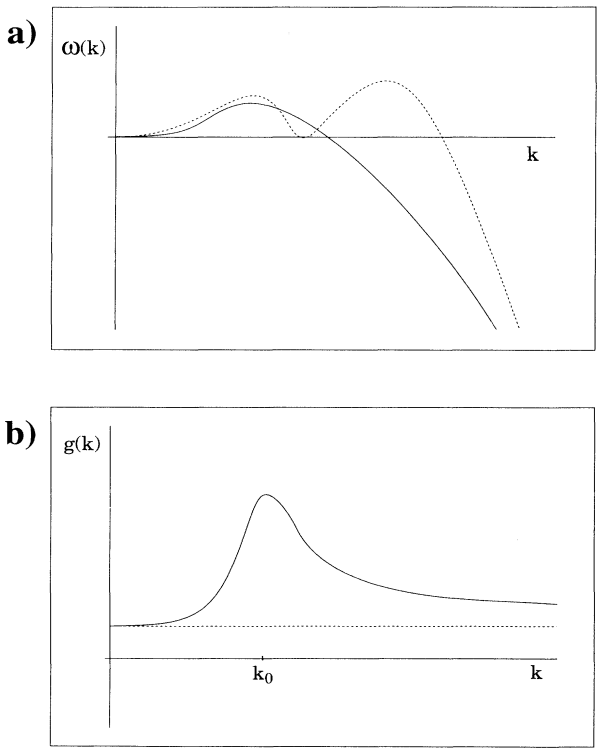

FIG. 5. (a) The solid line is a schematic representation of the dispersion relation for $\delta > \delta_c$. The dotted line shows the hypothetical form of the dispersion relation with two energy sources. (b) Proposed rate of energy mixing $g(k)$ that produces biscale patterns.

where the damping term can be rationalized in terms of the continuous spectrum of λ_i.

In the simulation of this equation we scale space, time, and ϕ_0 so that ν, κ, and $c/2$ are unity and take the following values for the parameters that appear in $g(k)$: $\epsilon = 0.2$, $k_0 = 0.6$, and $\gamma^2 = 0.005$. The results are presented in Fig. 4(b). In the figure one sees the existence of the structures with two different length scales, the main signature of biscale chaos. The generalized amplitude equation does not capture all of the details of cubic autocatalysis front dynamics far beyond the onset of instability. For example, the simulations of cubic autocatalysis show a broader distribution of longer length scales and, as is quite evident in Fig. 1, regions where there are no extrema. The full descriptions of these features may be specific to cubic autocatalysis and require a more detailed analysis. However, the main feature, the emergence of a second length scale, is described by the model.

We note the similarities in transitions to ordinary and biscale chaotic regimes. In the former case the transition takes place when $\langle \mathbf{u}_0|\mathbf{D}|\mathbf{u}_0\rangle$ passes through zero and in the latter we require a zero of $\{\delta_{ij}\lambda_i - \langle \mathbf{u}_i|\mathbf{D}|\mathbf{u}_j\rangle k^2\}$ to cross the real axis. The correspondence between the pole of $\widehat{\mathbf{W}}^{-1}$ and the existence of structures with different wave numbers suggests that this phenomenon can arise in other contexts. The existence of more complicated structures, say with three or four different wave numbers, is unlikely in view of the continuity of the spectrum and the fact that the dispersion relation is a smooth function of k. Consequently, the amplitude equation (19) could serve as the basis for the analysis of such phenomena in systems other than the cubic autocatalysis reaction.

IV. PARAMETERS IN THE KURAMOTO-SIVASHINSKY EQUATION

Thus far we have not related the parameters in the Kuramoto-Sivashinsky equation to those in the cubic autocatalysis model (1) and in this section we determine ν and κ. We first present an approximate analytical calculation of these parameters based on the exact solutions of the right and left eigenvalue problems for $|\mathbf{u}_0\rangle$ and $\langle \mathbf{u}_0|$, respectively, for the case of equal diffusion coefficients [20]. This provides insight into the structure of the eigenvalue spectrum and the corresponding eigenvalues. We then describe a general numerical scheme which can be applied to other models as well. In this section we choose a different space scaling and set $D_A = 1+\mu$ and $D_B = 1-\mu$ since this simplifies the computations.

A. Case of equal diffusion coefficients

When the diffusion coefficients are equal ($\mu = 0$) the reaction-diffusion equation (1) supports an additional relation involving the α and β concentrations due to conservation of the total mass at each point of space, $\alpha + \beta = 1$, given that at the initial time this relation is satisfied at every space point. We can rewrite system (1)

($D_A = D_B = 1$) in the form

$$\frac{\partial \alpha}{\partial t} = -\alpha(1-\alpha)^2 + \Delta\alpha \, . \tag{24}$$

Local initial input of the autocatalyst induces the creation of a front, propagating with the minimal velocity [8], whose profile is

$$\alpha_0(\xi) = [1 + \exp(-c\xi)]^{-1} \, , \tag{25}$$

where $c = 1/\sqrt{2}$ is the velocity of the front. The form of the β profile follows from the mass conservation relation. Henceforth, when confusion is unlikely to arise, we drop the subscript 0 on α and β to simplify the notation.

Next we discuss the spectrum of the eigenvalue problem (7) for the cubic autocatalysis problem when the diffusion coefficients are equal. Using the explicit form of $\mathcal{D}\mathbf{F}(\mathbf{z}_0)$ derived from (1) we have

$$\begin{aligned} \left(\frac{\partial^2}{\partial\xi^2} + c\frac{\partial}{\partial\xi} - \beta^2\right) X_1 - 2\alpha\beta X_2 &= \lambda X_1 \, , \\ \beta^2 X_1 + \left(\frac{\partial^2}{\partial\xi^2} + c\frac{\partial}{\partial\xi} + 2\alpha\beta\right) X_2 &= \lambda X_2 \, , \end{aligned} \tag{26}$$

where we have written the components of a general right eigenvector $\mathbf{u}$ as $\mathbf{u} = (X_1, X_2)$. We shall show that the spectrum is obtained from two distinct equations. First, by adding the two lines of (26), we obtain a linear differential equation with constant coefficients:

$$\left[\frac{\partial^2}{\partial\xi^2} + c\frac{\partial}{\partial\xi}\right] X = \lambda X \, , \tag{27}$$

where $X = X_1 + X_2$. After a change of variables $X = \exp(-c\xi/2)Y$ we obtain $\left[\partial^2/\partial\xi^2 - c^2/4\right] Y = \lambda Y$. The eigenvalue problem for Y has a continuous spectrum $\left(-\infty, -c^2/4\right]$. In these considerations we have omitted the case $X_1 + X_2 = 0$, which satisfies the eigenproblem for X automatically. Using this relation we obtain the following equation for the other part of the spectrum:

$$\left[\frac{\partial^2}{\partial\xi^2} + c\frac{\partial}{\partial\xi} + (2\alpha\beta - \beta^2)\right] X_1 = \lambda X_1 \, . \tag{28}$$

After the same change of variables $X_1 = \exp(-c\xi/2)Y_1$ we get a "Schrödinger" equation with potential $V = -2\alpha\beta + \beta^2$ [cf. Fig. 6(a)] and energy levels $E_i = -c^2/4 - \lambda_i$. We see that this equation has a continuous spectrum starting from zero as well as a discrete spectrum. The WKB method may be used to obtain approximations for the eigenvalues and eigenfunctions. Applying the Bohr-Sommerfeld quantization rule we get $E_0 = -0.1066$ for the first energy level, which is in good agreement with the theoretical value $-c^2/4 = -0.125$. This indicates that the WKB approximation is reliable and it predicts that the potential well is too shallow [21] to have other discrete energy levels. So we conclude that the spectrum consists of a zero eigenvalue and doubly degenerate continuous spectrum lying in $\left(-\infty, -c^2/4\right]$.

The right eigenvector $|\mathbf{u}_0\rangle = \partial|\mathbf{z}_0\rangle/\partial\hat{\xi}$ was discussed in Sec. II, but the left eigenvector $\langle\mathbf{u}_0|$ is more difficult to obtain. We now construct the explicit form for $\langle\mathbf{u}_0|$ for the case of equal diffusion. Letting $\langle\mathbf{u}_0|\xi\rangle = \mathbf{u}_0^*(\xi) = (X_1^*, X_2^*)$ the eigenvalue problem for $\mathbf{u}_0^*(\xi)$ takes the form

$$\begin{aligned} \left[\frac{\partial^2}{\partial\xi^2} - c\frac{\partial}{\partial\xi}\right] X_1^* - \beta^2(X_1^* - X_2^*) &= 0 \, , \\ \left[\frac{\partial^2}{\partial\xi^2} - c\frac{\partial}{\partial\xi}\right] X_2^* - 2\alpha\beta(X_1^* - X_2^*) &= 0 \, , \end{aligned} \tag{29}$$

so that the difference $X^* = X_1^* - X_2^*$ obeys

$$\left[\frac{\partial^2}{\partial\xi^2} - c\frac{\partial}{\partial\xi} + (2\alpha\beta - \beta^2)\right] X^* = 0 \, .$$

This can be cast into the form of (28) after the change of variable $X^* = A\exp(c\xi)Z$, where A is some constant defined by the normalization condition $\langle\mathbf{u}_0|\mathbf{u}_0\rangle = 1$:

$$\langle\mathbf{u}_0|\mathbf{u}_0\rangle = \int_{-\infty}^{\infty} \frac{\partial\alpha}{\partial\xi} X^* d\xi = cA\int_0^1 \alpha^2 d\alpha = \frac{cA}{3} \, ; \tag{30}$$

hence, we have

$$X^* = 3[1 + \exp(-c\xi)]^{-2} \, . \tag{31}$$

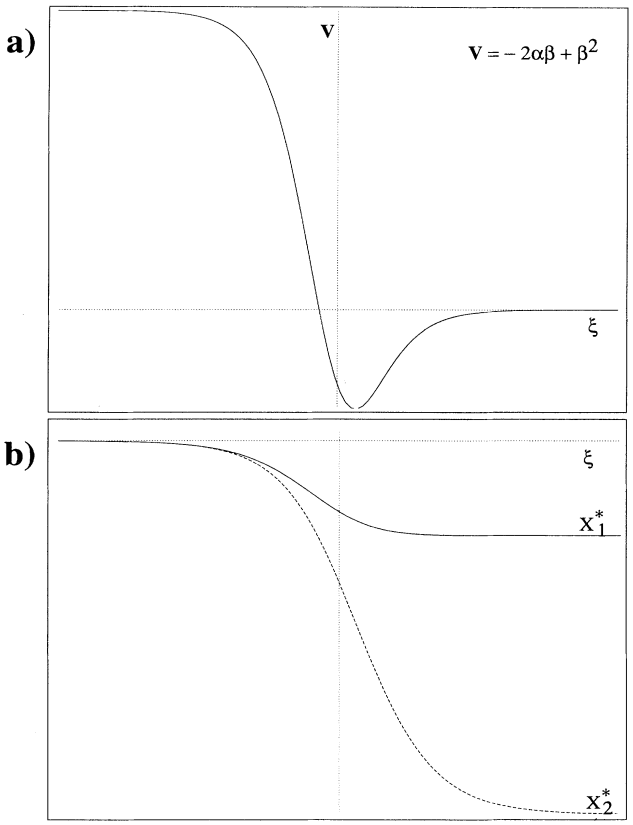

FIG. 6. (a) Plot of the potential in the WKB approximation. (b) Plots of the components of the left eigenvector for the case of equal diffusion coefficients.

Performing the change of variable $\Psi = \exp(-c\xi/2)X_1^*$ in (29) and using (31) we obtain

$$\frac{\partial^2}{\partial\xi^2}\Psi - \left(\frac{c}{2}\right)^2\Psi = 3\beta^2\exp(-c\xi/2)[1+\exp(-c\xi)]^{-2}\,. \tag{32}$$

The Green's function for the operator $[\partial^2/\partial\xi^2 - c^2/4]$ is given by $\mathcal{G}(\xi) = -c^{-1}\exp(-c|\xi|/2)$. Convolution of $\mathcal{G}$ with the right-hand side of (32) yields a solution for X_1^*,

$$X_1^*(\xi) = -\frac{1+2\exp(-c\xi)}{[1+\exp(-c\xi)]^2}\,, \tag{33}$$

and the difference between X_1^* and X^* gives X_2^*,

$$X_2^*(\xi) = -\frac{4+2\exp(-c\xi)}{[1+\exp(-c\xi)]^2}\,. \tag{34}$$

These functions are plotted in Fig. 6(b). The functions have limiting behavior $X_1^*(+\infty) = -1$ and $X_2^*(+\infty) = -4$.

System (29), for any diffusion coefficient ratio, has another zero left eigenfunction $\mathbf{V}^* = (1,1)$, which appears due to conservation of the total mass of the reagents. The right eigenfunction $\mathbf{V}$ corresponding to $\mathbf{V}^*$ is

$$V_1(\xi) = \frac{2}{3+3\exp(-c\xi)}\left(2+\frac{2c\xi+3}{1+\exp(c\xi)}\right)\,, \tag{35}$$

$$V_2(\xi) = 1-\frac{2}{3+3\exp(-c\xi)}\left(1+\frac{2c\xi+3}{1+\exp(c\xi)}\right)\,. \tag{36}$$

While both the "bra" vector corresponding to spatial invariance and the "ket" vector obtained above do not decay to zero at $\xi=\infty$ their scalar product does and the product is given, after change of variable, by

$$\langle\mathbf{V}|\mathbf{u}_0\rangle = \sqrt{2}\int_0^1\left[4\alpha^2\ln\frac{\alpha}{1-\alpha} - 2(1+3\alpha)(1-\alpha)\right]d\alpha = 0\,. \tag{37}$$

Since the above integral vanishes these considerations insure us that we have an orthogonal system of "bra" and "ket" vectors. Moreover, the fact that one product is finite and the other is not removes an ambiguity in the definition of the left eigenfunction. We believe the same situation holds for arbitrary μ.

1. Estimate of ν for $\mu \neq 0$

For equal diffusion coefficients $\mathbf{D}$ is the identity matrix and it follows that $\nu = \langle\mathbf{u}_0|\mathbf{D}|\mathbf{u}_0\rangle = 1$. However, using $|\mathbf{u}_0\rangle$ and $\langle\mathbf{u}_0|$ computed for $\mu=0$, we may obtain a first order approximation for ν for unequal diffusion coefficients. From (16) we write

$$\nu = \langle\mathbf{u}_0|\mathbf{D}|\mathbf{u}_0\rangle = 1+\mu\langle\mathbf{u}_0|\mathbf{I}|\mathbf{u}_0\rangle\,, \tag{38}$$

where $\mathbf{I} = \begin{pmatrix}1&0\\0&-1\end{pmatrix}$. Using the explicit, equal-diffusion forms for $\langle\mathbf{u}_0|$ and $|\mathbf{u}_0\rangle$ we get

$$\langle\mathbf{u}_0|\mathbf{I}|\mathbf{u}_0\rangle = \int_{-\infty}^{\infty}\frac{\partial\alpha}{\partial\xi}(X_1^*+X_2^*)\,d\xi = -\int_0^1(\alpha^2+4\alpha)\,d\alpha = -\frac{7}{3} \tag{39}$$

and $\nu = 1-7\mu/3$.

2. Estimate of κ for $\mu \neq 0$

When the diffusion coefficients are equal and $\mathbf{D}$ is the identity matrix we have $\kappa = 0$ in view of the orthogonality of the eigenfunctions. However, as in the preceding subsection we can obtain an estimate for κ for arbitrary μ using the solution of the eigenvalue problem for $\mu = 0$. To obtain this estimate we assert completeness of the set of eigenfunctions; i.e., $\sum_i |\mathbf{u}_i\rangle\langle\mathbf{u}_i| = \mathbf{1}$. Using this assumption we obtain [22]

$$\sum_i\frac{\langle\mathbf{u}_0|A|\mathbf{u}_i\rangle\langle\mathbf{u}_i|B|\mathbf{u}_0\rangle}{\lambda_i} = \langle\mathbf{u}_0|B|\mathbf{x}\rangle - \langle\mathbf{u}_0|B|\mathbf{u}_0\rangle\langle\mathbf{u}_0|\mathbf{x}\rangle\,, \tag{40}$$

where $|\mathbf{x}\rangle$ is a solution of the equation

$$\left[\mathcal{D}\mathbf{F} + \mathbf{D}\frac{\partial^2}{\partial\xi^2} + c\frac{\partial}{\partial\xi}\right]|\mathbf{x}\rangle = A|\mathbf{u}_0\rangle - \langle\mathbf{u}_0|A|\mathbf{u}_0\rangle|\mathbf{u}_0\rangle\,. \tag{41}$$

In this gereral expression we let $A = B = \mathbf{D}$ and use $\langle\mathbf{u}_0|\mathbf{D}|\mathbf{u}_i\rangle\langle\mathbf{u}_i|\mathbf{D}|\mathbf{u}_0\rangle = \mu^2\langle\mathbf{u}_0|\mathbf{I}|\mathbf{u}_i\rangle\langle\mathbf{u}_i|\mathbf{I}|\mathbf{u}_0\rangle$ in (41). Using $A = \mathbf{D}$ and adding the two lines of (41) we have

$$\left[\frac{\partial^2}{\partial\xi^2} + c\frac{\partial}{\partial\xi}\right](x_1+x_2) = 2\alpha_\xi\,, \tag{42}$$

with $\alpha_\xi = d\alpha/d\xi$. Solving the above equation with appropriate boundary conditions we get

$$x_1+x_2 = -\frac{2}{c}\frac{\ln(1+e^{c\xi})}{e^{c\xi}}\,. \tag{43}$$

Equation (41) can be solved for x_1 to obtain (we use in the next equation the explicit form for $\langle\mathbf{u}_0|\mathbf{I}|\mathbf{u}_0\rangle$)

$$\left[\frac{\partial^2}{\partial\xi^2} + c\frac{\partial}{\partial\xi} + 2\alpha\beta - \beta^2\right]x_1 = 2\alpha\beta(x_1+x_2) + \frac{10}{3}\alpha_\xi\,. \tag{44}$$

This equation takes an especially simple form after a change of variable $\xi\to\alpha$. The derivative possesses the form $(\partial/\partial\xi) = c\alpha(1-\alpha)(\partial/\partial\alpha)$ and (44) after simplifications is tantamount to

$$\alpha(1-\alpha)\frac{\partial^2}{\partial\alpha^2}x_1 + 2(1-\alpha)\frac{\partial}{\partial\alpha}x_1 + 2\left(3-\alpha^{-1}\right)x_1 = \frac{8}{c}\left(\frac{5}{12}+\frac{(1-\alpha)\ln(1-\alpha)}{\alpha}\right)\,. \tag{45}$$

We know that $\alpha\beta$ is a solution of the homogeneous equation. By the substitution $x_1 = \alpha\beta\chi$ we decrease the order of (44). Solving the resulting linear first order equation we obtain the solution

$$x_1 = \frac{2}{9c}\left[2\alpha^2(1-\alpha^2)\left(\ln(1-\alpha)+\alpha+\frac{\alpha^2}{2}\right)\alpha^2 + 7\alpha(1-\alpha)\ln\left(\frac{1-\alpha}{\alpha}\right)\right] . \quad (46)$$

From the form of the solution it is clear that the solution decays faster than $e^{-\gamma c|\xi|}$, $0 < \gamma < 1$, and thus the scalar product is well defined. To integrate we use the identity

$$\int_{-\infty}^{\infty} Q d\xi = \frac{1}{c}\int_0^1 \frac{Q}{\alpha(1-\alpha)} d\alpha , \quad (47)$$

and integration gives

$$\kappa = \sum_{i>0} \frac{\langle \mathbf{u}_0|\mathbf{D}|\mathbf{u}_i\rangle\langle \mathbf{u}_i|\mathbf{D}|\mathbf{u}_0\rangle}{\lambda_i} = \frac{264+40\pi^2}{27}\mu^2 . \quad (48)$$

Finally, collecting the above information, we arrive at the following expression for the Kuramoto-Sivashinsky equation with approximate coefficients deduced from the cubic autocatalysis model (1):

$$\frac{\partial\phi_0}{\partial t} = \left(1-\frac{7}{3}\mu\right)\nabla^2\phi_0 - \frac{264+40\pi^2}{27}\mu^2\nabla^4\phi_0 - \frac{c}{2}(\nabla\phi_0)^2 . \quad (49)$$

B. Numerical computation of ν for $\mu \neq 0$

In order to determine ν exactly, within the present approach, one must construct a scheme to determine the left eigenvector $\mathbf{u}_0^*$, the solution of $\mathcal{L}^\dagger\mathbf{u}^* = \lambda\mathbf{u}^*$, for $\lambda = 0$ and arbitrary μ. For the cubic autocatalysis problem the left eigenvectors are given by the solutions of

$$\left[(1+\mu)\frac{\partial^2}{\partial\xi^2} - c\frac{\partial}{\partial\xi} - \beta^2\right]\Psi_1 + \beta^2\Psi_2 = \lambda\Psi_1, \quad (50)$$

$$-2\alpha\beta\Psi_1 + \left[(1-\mu)\frac{\partial^2}{\partial\xi^2} - c\frac{\partial}{\partial\xi} + 2\alpha\beta\right]\Psi_2 = \lambda\Psi_2 ,$$

where we have written a general left eigenvector as $\mathbf{u}^* = (\Psi_1, \Psi_2)$. The solution of this eigenvalue problem in terms of a complete basis entails the solution of a difficult sparse, nonsymmetric, nontridiagonal matrix eigenvalue problem. In order to avoid solving the eigenvalue problem by matrix methods we use the following device. We consider an auxiliary problem that originates from the system of equations (50). In (50) we replace terms $c(\partial/\partial\xi)$ by the time derivative and take α and β to be in a moving frame with velocity $-c$ [i.e., $\alpha(t,x) = \alpha_0(x+ct)$, $\beta(t,x) = \beta_0(x+ct)$]:

$$\frac{\partial\Psi_1}{\partial t} = (1+\mu)\Delta\Psi_1 - \beta^2(\Psi_1 - \Psi_2), \quad (51)$$

$$\frac{\partial\Psi_2}{\partial t} = (1-\mu)\Delta\Psi_1 - 2\alpha\beta(\Psi_1 - \Psi_2) .$$

Eigenvalues of the adjoint eigenvalue problem $\mathcal{L}^\dagger\mathbf{u}^* = \lambda\mathbf{u}^*$ coincide with those of (7) and for nonzero eigenvalues their real parts are negative and separated from zero. Using this observation we deduce that all but one of the components exponentially decay so that the persistent solution of the system of partial differential equations (51) is proportional to $\langle\mathbf{u}_0|$. It is worth noting here that in order to obtain $\langle\mathbf{u}_0|$ one should take unequal initial distributions for Ψ_1 and Ψ_2 in (51).

Numerical computations of both (1) and (51) were carried out using the following hybrid of the Runge-Kutta and Crank-Nicholson methods:

$$\frac{\mathbf{z}'-\mathbf{z}(t)}{\tau} = \mathbf{D}\Delta\frac{\mathbf{z}'+\mathbf{z}(t)}{2} + \mathbf{F}(\mathbf{z}(t)) ,$$
$$\frac{\mathbf{z}(t+\tau)-\mathbf{z}(t)}{\tau} = \mathbf{D}\Delta\frac{\mathbf{z}(t+\tau)+\mathbf{z}(t)}{2} + \mathbf{F}\left(\frac{\mathbf{z}'+\mathbf{z}(t)}{2}\right) . \quad (52)$$

We use a nonuniform distribution of mesh points with density $x/(1-x^2)^{-1}$, where x is in the range $[-1,1]$. The matrix coefficients and vectors were computed using a finite element method with functions approximated by a sum of caret functions. During the simulations the profiles were monitored and constantly shifted to the origin. To do this the profiles were interpolated using a monotonicity-preserving, piecewise-cubic, Hermite interpolant to a set of data points [23]. For the velocity we use the following relation:

$$c = \int_{-\infty}^{\infty} \alpha\beta^2 d\xi . \quad (53)$$

Due to the fast decay of the rate of the reaction outside the reaction zone the infinite range of the integration can be replaced by the limit mesh points and the value of the definite integral of the interpolant is easily computed.

The results obtained in simulations for the case of equal diffusion coefficients were compared with the analytical results from the previous section. The absolute errors for the velocity and for $\langle\mathbf{u}_0|\mathbf{I}|\mathbf{u}_0\rangle$ are about 10^{-6} and 10^{-4}, respectively. This confirms that the numerical procedure is accurate.

V. CRITICAL DIFFUSION RATIO

While it is clear that the planar front is unstable for sufficiently large values of the diffusion ratio δ, no estimate was provided for the critical diffusion ratio, δ_c, where this instability takes place. There are a number of estimates of δ_c in the literature. Horváth *et al.* [10] estimated $\delta_c \approx 2.9$ from direct simulation of the reaction-

diffusion equation and found $\delta_c = 2$ from an application of Sivashinsky's method, which assumes an infinitely thin reaction zone, to the cubic autocatalysis problem. Zhang and Falle [24] computed the dispersion relation directly and found $\delta_c \approx 2.0$. Finally, Milton and Scott [25] obtained $\delta_c \approx 2.366$ using the eikonal theory and $\delta_c \approx 2.25$ from numerical simulation. This quantity is difficult to estimate by simulation of the reaction-diffusion equation and its direct calculation presents a number of interesting features.

In the context of the amplitude equations discussed in Sec. III, δ_c can be determined from the condition $\nu = \langle \mathbf{u}_0 | \mathbf{D} | \mathbf{u}_0 \rangle = 0$. This, in turn, requires the computation of the left and right eigenvectors of the eigenvalue problem [26]. The analytical estimate of ν discussed above immediately gives an estimate of the critical diffusion coefficient ratio. The critical value of μ, μ_c, is given by the solution of $\nu = 0 = 1 - 7\mu_c/3$ or $\mu_c = 3/7$. Since $\delta = (1+\mu)/(1-\mu)$ we have $\delta_c = 2.5$.

To determine the critical diffusion ratio exactly we use the numerical scheme outlined above to determine the left and right eigenvectors for arbitrary μ. In this way the critical diffusion ratio can be obtained iteratively. At each step the ratio from the previous run was taken and new profiles and the ratio $-\langle \mathbf{u}_0 | \mathbf{I} | \mathbf{u}_0 \rangle^{-1}$ corresponding to them were determined. Iterations rapidly converge to the value $\mu_c = 0.39397$, which corresponds to diffusion coefficient ratio $\delta_c = 2.300$.

We have also computed the dispersion relation to provide additional confirmation that $\delta_c > 2$. The details of the computation are given in the Appendix. The method we use allows us to put several thousand mesh points in the reaction zone (compared to about 40 in [24]). In the small wave number range the dispersion relation should have a dependence on k given by that of the Kuramoto-Sivashinsky equation. The maximum growth rate for the dispersion relation $\omega(k) = -\nu k^2 - \kappa k^4$ is $\nu^2/4\kappa$. We see that when δ approaches δ_c, so that $\nu \sim (\delta_c - \delta)$, the maximal growth rate rapidly decreases and can easily fall out of range of the precision of the calculation. Moreover, direct simulation shows the presence of a very slowly decaying tail of the autocatalyst and its length increases (cf. the Appendix) when k approaches zero. So the calculations could also be affected by the limited system size. We also observe that least-squares fittings of the data in Fig. 2(a) of [24] gives $\nu = 0.34$ and $\kappa = 1.7$ indicating stability of the front. A further test of our computation of the dispersion relation comes from the first order approximation of ν in the Kuramoto-Sivashinsky equation when $\mu \approx \mu_c$: $\mu = \mu_c + \delta\mu$. In this case we have $\nu = 1 + \mu\langle \mathbf{u}_0 | \mathbf{I} | \mathbf{u}_0 \rangle = -\delta\mu/\mu_c$. The results of our computations of the dispersion relation for the case $\mu = 0.45$ ($\delta = 2.636$) are given in Fig. 7. We see that near the origin the dispersion relation is well approximated by the curve $\omega = 0.142k^2$, where $0.142 = \delta\mu/\mu_c$.

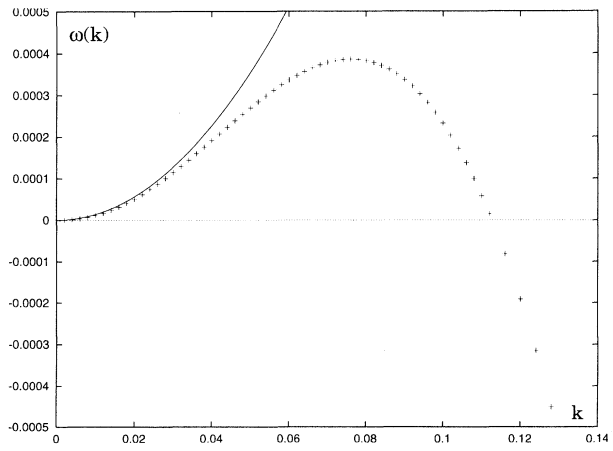

FIG. 7. Dispersion relation of the cubic autocatalysis model for the case $\mu = 0.45$ (or $\delta = 2.636$). The symbols + denote the dispersion relation constructed from the numerically obtained growth rate. It is compared with the first order approximation $\omega(k) \approx 0.142k^2$ for small values of k.

VI. SUMMARY AND DISCUSSION

The chaotic dynamics of cubic autocatalysis fronts shows two distinct kinds of behavior depending on the diffusion ratio D_A/D_B. Close to the onset of the front instability the transverse structure can be described in terms of a single length scale. The characteristic length is associated with the wavelength of the most unstable mode and the dynamics can be viewed in terms of a particle picture. The front extrema can be associated with "particles" that collide and coalesce and new particles are created to maintain the average particle number. This dynamical regime was characterized statistically and shown to be described by the Kuramoto-Sivashinsky equation.

For large values of D_A/D_B a dynamical regime was found where the front is characterized by two length scales. We term this type of chaotic front dynamics biscale chaos. Biscale chaos cannot be described by the Kuramoto-Sivashinsky equation and we introduced an amplitude equation which is a generalization of this equation. This amplitude equation accounts for a modified nonlinear energy mixing among the modes. We identified this kind of behavior with a pole near the real axis of a linear operator obtained in the course of the analysis of the dynamics of small perturbations. The observed phenomenon may prove to be quite general in light of the simple prerequisite for it, namely, the crossing of the real axis by a pole. However, we believe that the coexistence of structures with three or more length scales is unlikely since it requires the operator to have more complicated properties. Questions about qualitative effects of this irregular dynamics on microscopic quantities (e.g., mean front velocity, diffusion coefficient of the interface, etc.) remain. Another point to be investigated is the possibility of describing the observed patterns in terms of the dynamics of interacting pulses, which correspond to small k modes, driven by noise.

An explicit reduction of the cubic autocatalysis reaction-diffusion equation to the Kuramoto-Sivashinsky equation was carried out and the coefficients that en-

ter in this equation were determined. Both approximate analytical values as well as a numerical scheme for their exact computation for arbitrary D_A/D_B were given. The numerical method copes with two problems that arise in such calculations, namely, the nonlocal form of the zero eigenvector and the degeneracy of the eigenproblem with eigenvalue equal to zero, which comes from the conservation laws for the system. The algorithm is easy to implement and proved to be reliable. Using these results the critical diffusion ratio where the front instability occurs was computed and found to be $D_A/D_B = 2.300$.

ACKNOWLEDGMENTS

This work was supported in part by a grant from the Natural Sciences and Engineering Research Council of Canada. A. Careta benefitted from a fellowship of the Programa de Becas de Formación de Personal Investigador en el Extranjero, Ministerio de Educación y Ciencia, Spain.

APPENDIX: NUMERICAL COMPUTATION OF THE DISPERSION RELATION

The dispersion relation for the cubic autocatalysis model was computed in the following way: The perturbation of the front solution of (5) may be written in the form

$$\mathbf{z}(t,x,y) = \mathbf{z}_0(\xi) + \boldsymbol{\chi}(t,x)\exp(\imath k y) \; . \qquad \text{(A1)}$$

We assume, when k is small, that the largest eigenvalue is separated from the others. Thus, after integration of the equation

$$\frac{\partial \boldsymbol{\chi}}{\partial t} = \mathcal{D}\mathbf{F}\boldsymbol{\chi} + \mathbf{D}\left(\frac{\partial^2}{\partial x^2} - k^2\right)\boldsymbol{\chi} \; , \qquad \text{(A2)}$$

for a sufficiently long time, only the most unstable mode survives. The system (A2) is the same as system (4.7) of [24] after proper scaling and change of variables $\chi_1 = a_1 - da_0/dx$, $\chi_2 = b_1 - db_0/dx$ in the notation of this paper [27]. After transients the solution of (A2) should propagate with the same velocity as the front and grow with a rate $\omega(k)$ and thus we can replace $\partial\boldsymbol{\chi}/\partial t$ with $\omega(k)\boldsymbol{\chi} - c\boldsymbol{\chi}_\xi$. In [24] the eigenvalue problem with $\boldsymbol{\chi}$ as a vector and $\omega(k)$ as eigenvalue was solved. The two approaches lead to the same result but the latter necessitates solving an eigenvalue problem for a nonsymmetric, sparse matrix that is in general a difficult task. The direct integration of the system (A2) is more accurate and easier to implement. The results of the integration for $\mu = 0.45$ are shown in Fig. 7.

To decrease the integration time we used as initial conditions for $\boldsymbol{\chi}$ the eigenvector obtained from the run for $k - \delta k$ and by employing numerical differentiation we computed $|\mathbf{u}_0\rangle$, which is solution of the eigenvalue problem for $k = 0$.

We also note that the autocatalyst exhibits a slowly decaying tail whose length increases as k approaches zero. The length of the tail can be estimated from the equation, $\chi_2'' = k^2\chi_2 - c(1-\mu)^{-1}\chi_2'$, which is obtained from the equation governing the dynamics of the autocatalyst [second member of (A2)] by setting the reaction terms to zero. When k is small the solution exponentially decays as $\exp[-(1-\mu)k^2x/c]$ and the length of the tail is of order $L_{\mathrm{ta}} \sim c[(1-\mu)k^2]^{-1}$.

[1] See, for instance, A.-L. Barabási and H. E. Stanley, *Fractal Concepts in Surface Growth* (Cambridge University Press, Cambridge, 1995).
[2] *Non-Steady Flame Propagation*, edited by G. H. Markstein (Macmillan, New York, 1964).
[3] See, for example, A. Arneodo and J. Elezgaray, in *Chemical Waves and Patterns*, edited by R. Kapral and K. Showalter (Kluwer, Dordrecht, 1995), p. 517; A. Hagberg and E. Meron, Phys. Rev. Lett. **72**, 2494 (1994).
[4] See G. I. Sivashinsky, Annu. Rev. Fluid Mech. **15**, 179 (1983), and references therein.
[5] D. Horváth and K. Showalter, J. Chem. Phys. **102**, 2471 (1995).
[6] Y. Kuramoto and T. Tsuzuki, Prog. Theor. Phys. **55**, 356 (1976).
[7] G. I. Sivashinsky, Combust. Sci. Tech. **15**, 137 (1977).
[8] J. Billingham and D. J. Needham, Philos. Trans. R. Soc. Ser. A **334**, 1 (1991).
[9] S. K. Scott and K. Showalter, J. Phys. Chem. **96**, 8702 (1992).
[10] D. Horváth, V. Petrov, S. K. Scott, and K. Showalter, J. Chem. Phys. **98**, 6332 (1993).
[11] These plots were produced by an Euler integration of (1) with space and time steps Δr and Δt, selected to insure numerical stability and convergence, which was verified by varying these parameters. Typical values are $\Delta r = 2$ and $\Delta t = 0.5$ or 0.1. In order to mimic a system infinite in the x direction, the lattice was shifted to compensate for the front motion so that the interface was always contained in the finite integration domain.
[12] Y. Kuramoto, *Chemical Oscillations, Waves, and Turbulence* (Springer-Verlag, New York, 1984).
[13] From the assertion about the stability of the one dimensional problem we have $\mathrm{Re}(\lambda_i) < \sigma < 0$ and we see that, for small values of ν in the Kuramoto-Sivashinsky equation, $k \sim \langle \mathbf{u}_0|\mathbf{D}|\mathbf{u}_0\rangle^2$ is also small and the procedure is self-consistent in this limit.
[14] See also, T. Bohr and A. Pikovski, Phys. Rev. Lett. **70**, 2892 (1993).
[15] V. Yakhot, Phys. Rev. A **24**, 642 (1981).
[16] M. Kardar, G. Parisi, and Y.-C. Zhang, Phys. Rev. Lett. **56**, 889 (1986).
[17] I. Procaccia, M. H. Jensen, V. S. L'vov, K. Sneppen, and R. Zeitak, Phys. Rev. A **46**, 3220 (1992).
[18] K. Sneppen, J. Krug, M. H. Jensen, C. Jayaprakash, and T. Bohr, Phys. Rev. A **46**, R7351 (1992).
[19] S. Zaleski, Physica D **34**, 427 (1989).
[20] Koga and Kuramoto [Prog. Theor. Phys. **63**, 106 (1980)]

carried out a stability analysis of the stationary, localized solution of the FitzHugh-Nagumo model. In this case the solutions of the adjoint problem are also localized and no difficulties are encountered. In the stability analysis of a propagating front the left eigenvector does not necessarily decay as distances tend to infinity. There is another problem arising from the chemical nature of the model: the reaction-diffusion equation possesses an additional zero left eigenvector due to the conservation of the reagents and no recipe is given for how to choose the correct one.

[21] Integration of the Bohr momentum over the allowable domain yields 3.1 when the next value in quantization rule is $3\pi/2 \approx 4.5$.

[22] We write $|\mathbf{x}\rangle$ as $|\mathbf{x}\rangle = \sum_{i>0} \eta_i |\mathbf{u}_i\rangle$ so that $[\mathbf{A}|\mathbf{u}_0\rangle - \langle \mathbf{u}_0|\mathbf{A}|\mathbf{u}_0\rangle|\mathbf{u}_0\rangle] = \sum_{i>0} \lambda_i \eta_i |\mathbf{u}_i\rangle$. $\langle \mathbf{u}_0|\mathbf{B}|\mathbf{x}\rangle$ is replaced by $\sum_{i>0} \eta_i \langle \mathbf{u}_0|\mathbf{B}|\mathbf{u}_i\rangle$ but $\lambda_i \eta_i = \langle \mathbf{u}_i|\mathbf{A}|\mathbf{u}_0\rangle$, thus proving the statement.

[23] In the simulations we used the NAG library for numerical analyses. Linear equations were solved using the NAG library routine F04FAF. For interpolation we employed subroutine E01BEF which computes a monotonicity-preserving, piecewise-cubic, Hermite interpolant to a set of data points. The value of the definite integral of the interpolant was determined using E01BHF.

[24] Z. Zhang and S. A. E. G. Falle, Proc. R. Soc. London Ser. A **446**, 1 (1994).

[25] R. A. Milton and S. K. Scott, J. Chem. Phys. **102**, 5271 (1995).

[26] One may be tempted to look for the stability of the system with respect to some class of perturbations and thus avoid computation of the left zero eigenvector. In this case the value obtained is unpredictable. Take, for example, a perturbed solution in the form $\mathbf{z}(t,x,y) = \mathbf{z}_0(x - ct + \boldsymbol{\eta}(\mathrm{t,y}))$ for the cubic autocatalysis model. Expanding Eq. (1) in a power series in $\boldsymbol{\eta}$ and integrating over all x we arrive at the set of equations

$$\begin{aligned} \partial\eta_1/\partial t &= A(\eta_1 - \eta_2) + D_A \Delta\eta_1, \\ \partial\eta_2/\partial t &= A(\eta_1 - \eta_2) + D_B \Delta\eta_2 , \end{aligned}$$

where A is some positive constant and we have used $\int 2\alpha\beta\beta_\xi d\xi = -\int \beta^2 \alpha_\xi d\xi$. The above system loses stability whenever $D_A > D_B$ and it is obvious that this value does not coincide with the critical diffusion coefficient ratio.

[27] We use the set of identities

$$\begin{aligned} -c\alpha_\xi &= (1+\mu)\alpha_{\xi\xi} - \beta^2\alpha_\xi - 2\alpha\beta\beta_\xi, \\ -c\beta_\xi &= (1-\mu)\beta_{\xi\xi} + \beta^2\alpha_\xi + 2\alpha\beta\beta_\xi \end{aligned}$$

obtained by differentiation of the front solution. We find the system (A2) to be more compact when we use this particular form of the perturbation.